Strojnícky časopis – *Journal of* MECHANICAL ENGINEERING,
VOL 72 (2022), NO 2, 139 - 148

APPLICATION OF A NOVEL METHODOLOGY FOR THE DETECTION OF HARMONIC VIBRATION IN THE ACCELERATION-TIME FUNCTIONS OF VEHICLE PLATFORMS

PIDL Renáta[1]

[1] Department of Applied Mechanics, Faculty of Mechanical Engineering, Informatics and Electrical Engineering, Széchenyi István University, Egyetem tér 1, H-9026 Győr, Hungary, e – mail: pidlre@sze.hu

Abstract: In this paper, an attempt is made to determine whether Cepstrum analysis can be applied to detect pure harmonic sine waveform acceleration-time signals in a frequency sub-band from the acceleration-time function of vehicle load platforms. Based on Cepstrum evaluation of specific measurement results at different speeds and under different road conditions, the analysis reveals that no frequency band exhibits full-period pure sinusoidal excitation, which casts doubt regarding usuage of sinusoidal sliding frequency tests for package shaking tests.

KEYWORDS: vehicle dynamics, resonance phenomena, FFT analysis, Cepstrum analysis, vibration acceleration measurement, acoustics

1 Introduction

The vibration loads arising during transport and goods handling show a very wide variation depending on the conditions of the road-vehicle systems [1-10]. The Lansmont vibration measuring and recording instrument available in our laboratory was deployed with loads, partly in containers, partly in railcars and partly in a wide variety of transport modes. The first task which has to be investigated is the choice of parameters for the digital instrument setup in order to reliably record the acceleration-time functions to be recorded, in order to generate a reliable function stream of the entire transport process, which can take weeks or even months. For this part of the study, the use of sampling theorem (mainly Shannon's theorem) from the field of digital signal processing has to be investigated [11]. Also, the problem of optimal choice of the so-called Nyquiest limit is to be investigated, since this limit affects the spectrum of the acceleration-time function for higher frequency harmonic signals. Sometimes, higher frequency signals are introduced into the spectra below the Nyquiest limit, increasing the value of the low frequency acceleration amplitudes [12]. This phenomenon can in principle be avoided by choosing the right anti-aliasing filter during signal acquisition. Already at the signal acquisition stage, care must be taken to determine which frequency bands are relevant for the signal and to set the low-pass and high-pass filter values and the narrow-band filter series. Choosing this is very difficult and it has to be investigated until the original acceleration-time function by back-transforming the filtered spectrum is obtained. It is equally important to avoid the so-called spectral leakage.

If frequency components are found in the period of the acceleration-time function whose period time does not give an integer quotient, then the period of the extracted acceleration-time function is divided and the spectral leakage occurs. This means that when these sections are coupled together, a leap occurs in the function at each fit. Spectral leakage can only be determined by continuous analysis of the recorded data and iteration. The possibility of using

DOI: 10.2478/scjme-2022-0024, Print ISSN 0039-2472, On-line ISSN 2450-5471

different window functions should also be investigated to prevent spectral leakage. In the Matlab software, there are several smoothing window functions for the stochastic function, and it will be experimented with trying them out in a first approximation (Shannon, Hamming, etc.)

In the evaluation, the focus should be placed on the application of the discrete Fourier transform, which gives energy spectra in narrow intervals by incorporating the Parseval theorem [13]. The Wiener-Hincsin theorem [14,15], which is the transform of the autocorrelation function from the acceleration time function must be applied. It need to be investigated how well the two functions formed from the autocorrelation functions satisfy the linearity theorem. It also need to be examined the convolution spectrum to see if the convolution of the two signals is equal to the inverse Fourier transform of the product of the spectra of the two signals taken separately. Practically, this can be applied to the transfer function of the load platform - loads, if my assumption is satisfied. Finally, it has to be considered that frequency modulation can simplify the evaluation if a modulated frequency signal can be found. Based on the functions thus evaluated, the tuning limits of modern shaking simulators, frequency sweep rates, etc. can be better approximated to reality. From a vibration-engineering point of view, the critical frequency bands are those at which a full-period harmonic excitation signal appears. At these frequencies, there is a chance that this harmonic full-period sine wave signal will meet the natural frequency of the load or its components on the vehicle platform, and in this case, even in a very short time, resonance may occur, i.e. a 5 to 20 times gain compared to the input signal may occur in the response signal. In fact, the efficiency of the shake table test can be increased by exposing the packaged product sample to only these frequency bands and detecting whether resonance occurs at these frequencies.

2 Determining the properties of the acceleration-time function recorded on a vehicle platform using cepstrum analysis

The cepstrum function is generated from the original signal as follows:

$$c[n] = \mathcal{F}^{-1}\{\log|\mathcal{F}\{x[n]\}|\}, \tag{1}$$

where $\mathcal{F}$ is the DFT and $\mathcal{F}^{-1}$is the IDFT. The cepstrum is:

$$c[n] = \sum_{n=0}^{N-1} \log\left(\left|\sum_{n=0}^{N-1} x[n]e^{-j\frac{2\pi}{N}kn}\right|\right) e^{j\frac{2\pi}{N}kn}. \tag{2}$$

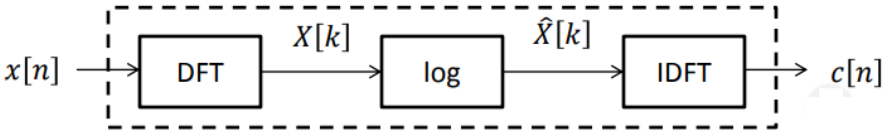


Fig. 1 Flowchart of the Cepstrum analysis

So the raw acceleration-time function must take the Fourier transform, and then the logarithm of this. Finally, the resulting logarithm spectrum is inverse-Fourier transformed to obtain the Cepstrum function.

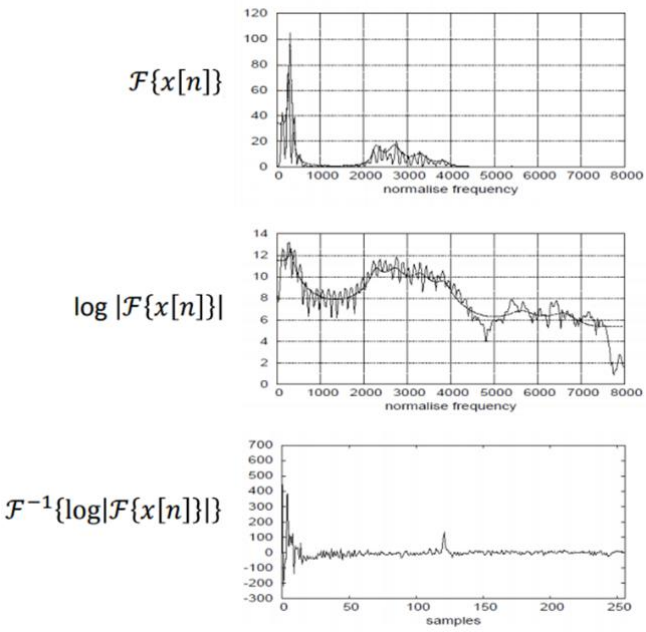


Fig. 2 Functions of each component

Fig. 2 shows that the original spectrum (top graph) is very sideband. The logarithm of the spectrum tends to highlight these sidebands at narrow bands of latitude where the spectrum would otherwise take low values.

If the inverse Fourier transform of the logarithmic spectrum is taken, the Cepstrum function will be obtained. One peak can be observed in the cepstrum function (except for values of the function near 0) at ~120 samples in the figure above. This peak is present due to the sidebanding.

By imagining the logarithmic spectrum as an acceleration-time function and then the inverse Fourier transform trained from it, there should be a peak on the cepstrum where the transform finds a "harmonic", exactly such a peak is also due to the sidebanding, since this is perceived as a harmonic by the transform. The density of the sideband is indicated by the value of the cepstrum function on the horizontal axis at the peak. This is called "quefrency", in the frequency pattern, and is measured in [ms] or [s] (time). By examining the value of the cepstrum at the peak and then taking the reciprocal of this value (if secundum), it is possible to obtain the frequency spacing of the sideband across the spectrum.

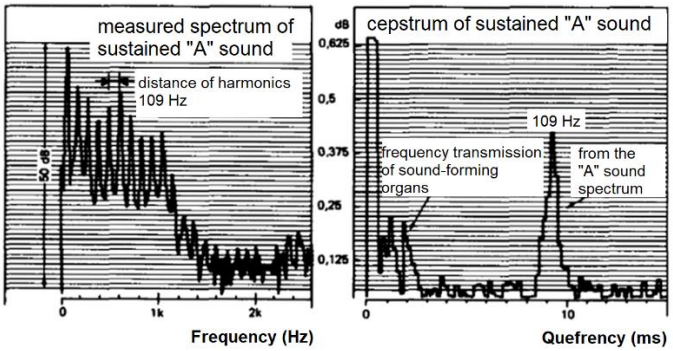


Fig. 3 Acoustic application of cepstrum analysis

Fig. 3 clearly shows the side-banding of the spectrum and that there is a peak in the cepstrum function at about 9 milliseconds. The reciprocal of 9 ms is exactly:

$$\frac{1}{1 \cdot 10^{-3}} = \frac{1000}{9} = 111 \text{ Hz} \tag{3}$$

With a small error (since the peak is not exactly at 9), the density of the sidebands can be obtained. The low quefrency parts of the cepstrum function are due to amplitude modulation. If these two domains could be separated by filtering, then the harmonic components could be determined (Fig. 4).

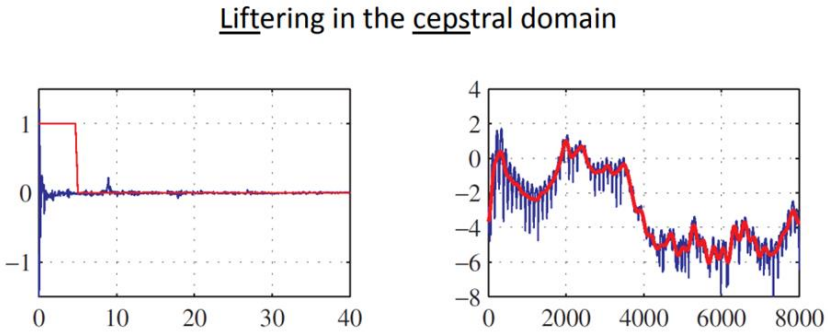


Fig. 4 Influence of liftering on the cepstrum value

It can be seen that the left cepstrum function is filtered ("liftering" is filtering here) so that the quefrency peak is weighted zero. By transforming this back, we get back a kind of envelope curve of the spectrum.

The cepstrum function is filtered so that low quefrency parts are identified by transmission and high quefrency parts by excitation (Fig. 5).

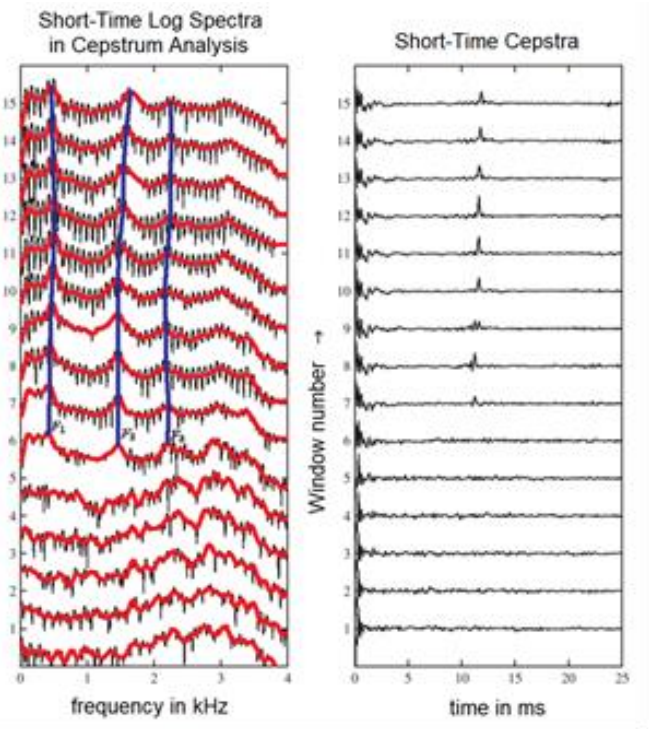


Fig. 5 Variations of cepstrum functions as a function of spectra

3 Evaluation of own measurements with Cepstrum analysis

3.1 Measurement conditions

The test consignment

Lorry:

- Renault semi-trailer tractor (280 kW, diesel),
- Maximum towable mass: 33 480 kg.

Semi-trailer:

- Wilkien Oldenburt,
- Suspension: air spring.

Load (Fig. 6):

- 14 multi-way engine mount pallets (528 898), weight: ~400 kg/each,
- 3 EA 837 Gen3 Q5 engines, weight: 174 kg/each,
- 3 EA 837E EVO B8/C7/D4 motors, weight: 184 kg/db,
- Total load weight: 6 674 kg.



Fig. 6 The test load with the measuring instrument

3.2 The measuring instrument

A SAVER 3X90 Shock and Vibration data logger was used for the measurement (Fig. 7). The results were evaluated using Xware software and MATLAB R2014a for filtering conditions and Fourier calculations.

The measuring device is equipped with a built-in three-way piezoelectric acceleration sensor. A lithium-ion battery was used to record and store sufficient data. The resulting accelerations and shaking events were recorded in both the vertical, transverse and longitudinal directions. Data are presented in Central European time zone.

The position of the instrument was chosen to ensure that the recorded acceleration signals were as close as possible to the engine (while at the same time not damaging the instrument in the event of a possible movement out of the nest). The position of the instrument is illustrated in Fig. 6.



Fig. 7 The measuring and recording instrument used

3.3 Measurement results

Fig. 8 shows the PSD and the cepstrum function of driving on a motorway at 60 km/h.

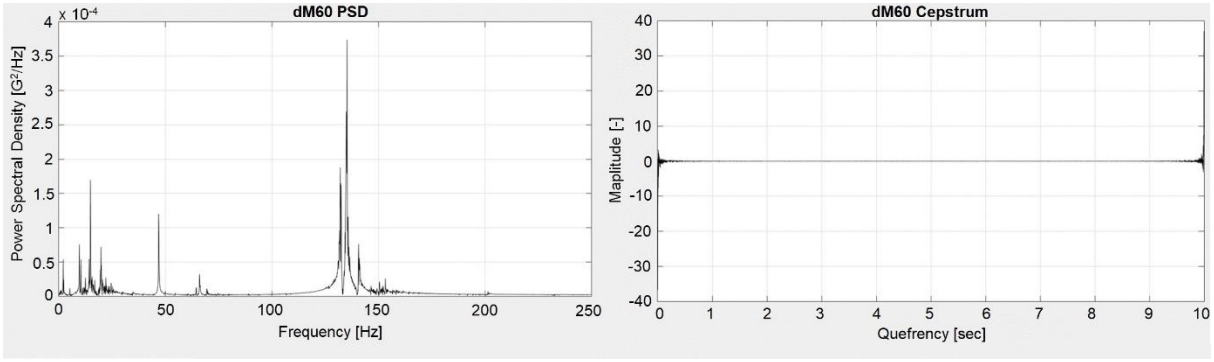


Fig. 8 Motorway 60 km/h speed (dM60) PSD and the resulting cepstrum function (no frequency modulation)

Fig. 9 shows the cepstrum function from the PSD of driving on the motorway at 60 km/h (dM60) magnified.

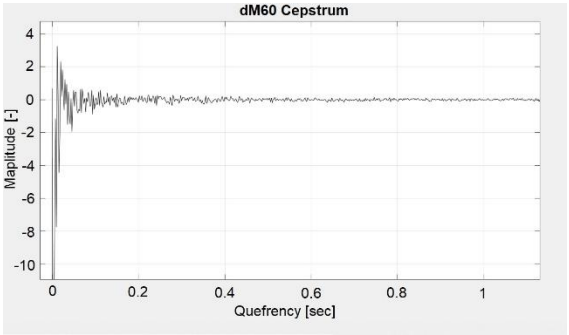


Fig. 9 Cepstum function of Fig. 8 zoomed in

Transformed into the frequency domain, this means that there is a large amplitude of acceleration in the region around 0.2 Hz. The surface of the vehicle is almost undulating.

Otherwise, all cepstrum functions are strongly tending to 0 around the Nyquist quefrency, which is at 5 seconds.

Fig. 10 shows the PSD and the cepstrum function of driving on the motorway at 70 km/h (dM70).

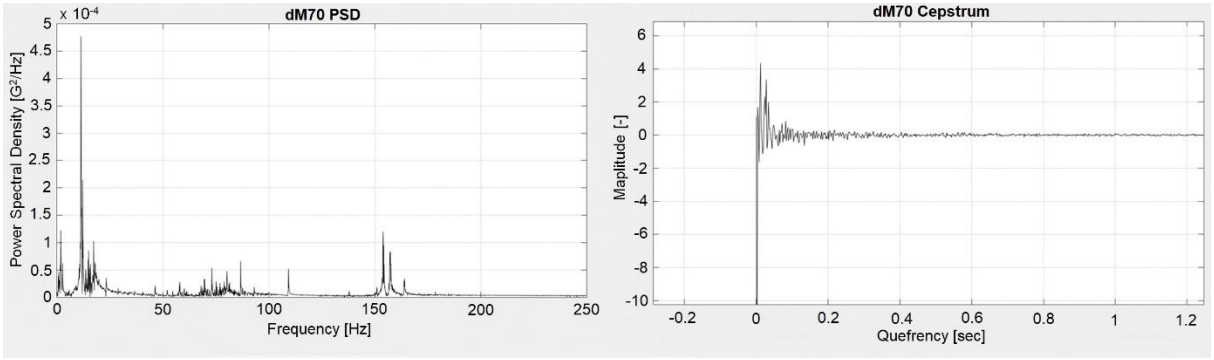


Fig. 10 Motorway 70 km/h speed (dM70) PSD and derived cepstrum function (no frequency modulation)

Fig. 11 shows the PSD and the cepstrum function of driving on a motorway at 80 km/h (dM80).

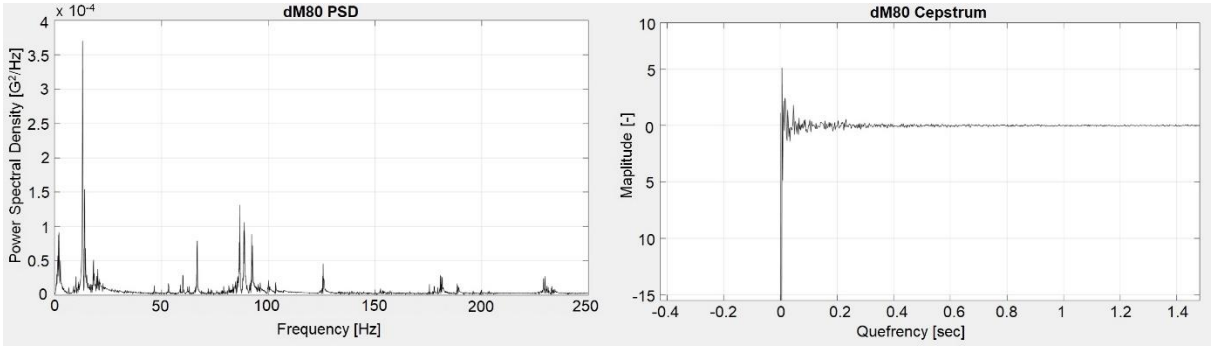


Fig. 11 Motorway 80 km/h speed (dM80) PSD and derived cepstrum function (no frequency modulation)

Fig. 12 shows the PSD and the cepstrum function of driving on the motorway at 90 km/h (dM90).

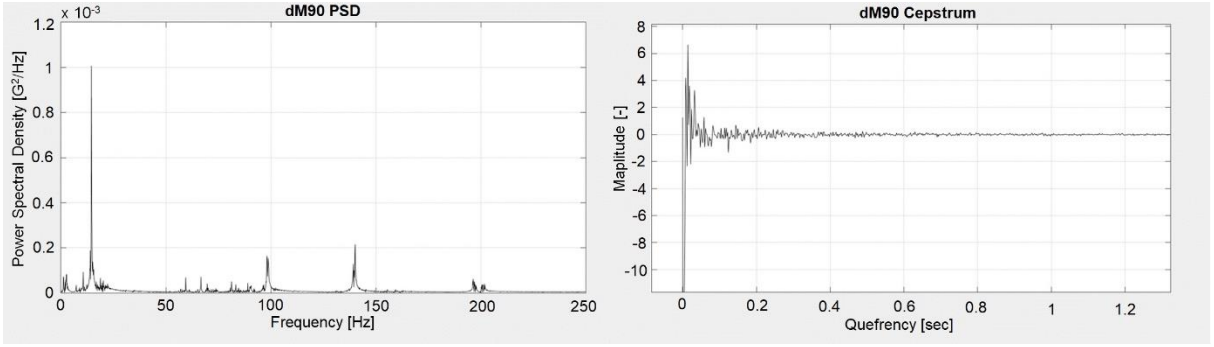


Fig. 12 Motorway 90 km/h speed PSD (dM80) and derived cepstrum function (no frequency modulation)

Fig. 13 shows the PSD and the resulting cepstrum function for a territorial road at 40 km/h (dT40).

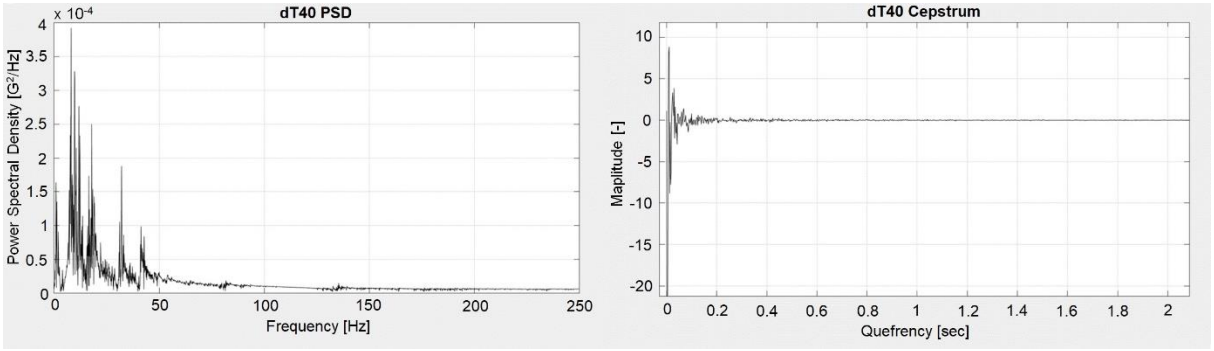


Fig. 13 Territorial road 40 km/h speed (dT40) PSD and derived cepstrum function (no carrier frequency)

Fig. 14 shows the PSD and the resulting cepstrum function of driving on a territorial road at 60 km/h (dT60).

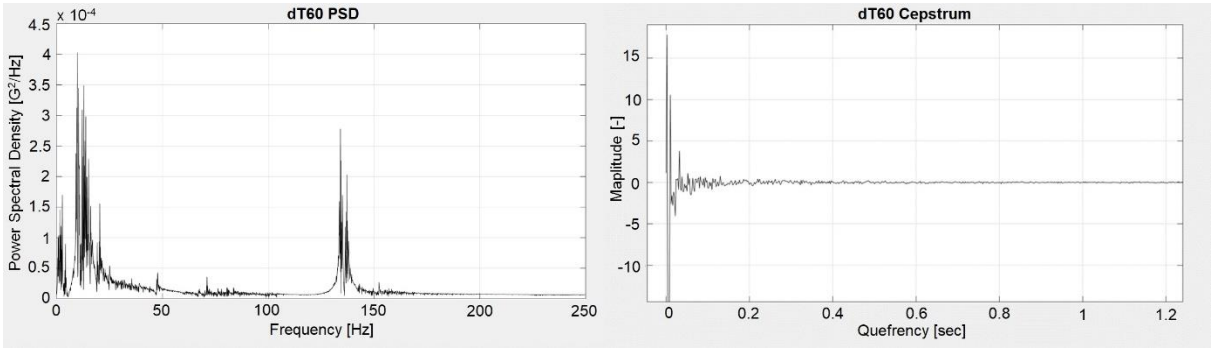


Fig. 14 Territorial road 60 km/h speed (dT60) PSD and derived cepstrum function (no carrier frequency)

Fig. 15 shows the PSD and its cepstrum function for a teritorial road at 80 km/h (dT80).

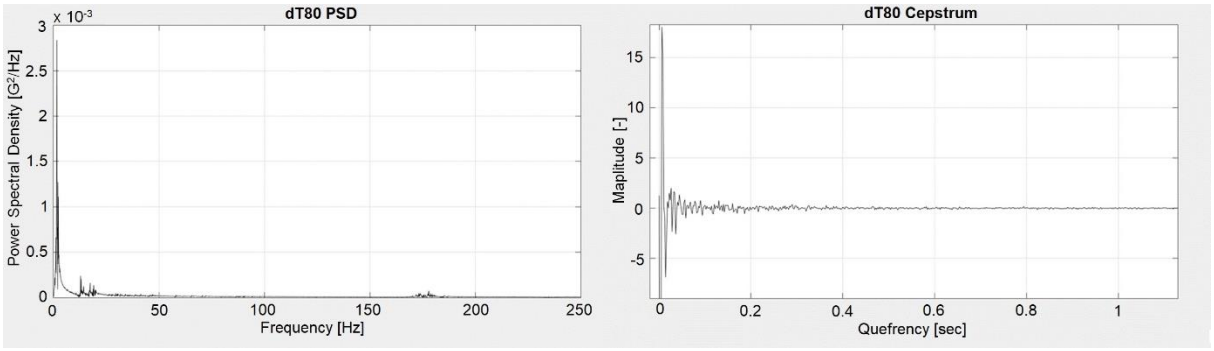


Fig. 15 Territorial road 80 km/h speed (dT80) PSD and derived cepstrum function (no carrier frequency)

CONCLUSION

The Cepstrum analysis shows that harmonic excitation occurs only in the 0-0.2 Hz range, regardless of the path conditions. The analysis also shows that for identical road conditions, there is always a travel speed at which the maplitudo (amplitude inverse) is the smallest and it would be advisable to travel at this speed. In practice, the reality of this is low, because road vehicles have to fit into the traffic. A further lesson is that the phenomenon of optimum speed can be observed on poor road conditions, but this is significantly dependent on road conditions. For road defects with a larger longitudinal extent, a low speed is recommended, while for road defects with a smaller longitudinal extent, a higher speed is recommended.

Above frequencies of 0.2 Hz, harmonic oscillations, which are considered to be relatively long-lived, are excluded.

REFERENCES

[1] Charles, D. “Derivation of environment descriptions and test severities from measured road transportation data”, Journal of the IES 36(1), pp. 37 – 42, **1993**. DOI: 10.17764/jiet.2.36.1.k285j24551552377

[2] Chonhenchob, V., Singh, S.P., Singh, J., Stallings, J., Grewal, G. “Measurement and Analysis of Vehicle Vibration for Delivering Packages in Small-Sized and Medium-Sized Trucks and Automobiles”, Packaging Technology and Science 25(1), pp. 31 – 38, **2012**. DOI: 10.1002/pts.955

[3] Chonhenchob, V, Singh, S.P., Singh, J., Sittipod, S., Swasdee, D., et al. “Measurement and analysis of truck and rail vibration level in Thailand”, Packaging Technology and Science, 23, pp. 91 – 100, **2010**. DOI: 10.1002/pts.881

[4] Garcia-Romeu-Martinez, M. A., Singh, S.P., Cloquell-Ballester, V.A. “Measurement and analysis of vibration levels for truck transport in Spain as a function of payload, suspension and speed”, Packaging Technology and Science 21(8), pp. 439 – 451, **2008**. DOI: 10.1002/pts.798

[5] Böröcz, P. “Averaged vibration levels during courier parcel delivery service in small truck in Hungary”, FME Transaction 46(2), pp. 211 – 217, **2018**. DOI: 10.5937/fmet1802211B

[6] Matijević, D. V., Popović, V. M. “Overview of Modern Contributions in Vehicle Noise and Vibration Refinement with Special Emphasis on Diagnostics”, FME Transactions 45(3), pp. 448 – 458, **2017**. DOI: 10.5937/fmet1703448M

[7] Danko, J., Milesich, T., Bucha, J. "Nonlinear Model of the Passenger Car Seat Suspension System", Strojnícky časopis – Journal of Mechanical Engineering 67(1), pp. 23 – 28, **2017**. DOI: 10.1515/scjme-2017-0002

[8] Likaj, R., Shala, A. "Optimisation and Control of Vehicle Suspension Using Linear Quadratic Gaussian Control", Strojnícky časopis – Journal of Mechanical Engineering, 68(1), pp. 61 – 68, **2018**. DOI: 10.2478/scjme-2018-0006

[9] Pavlo, M., Oleksii, L., Vadym, S. "Approximate Calculation of the Natural Oscillation Frequency of the Vibrating Table in Inter-Resonance Operation Mode", Strojnícky časopis – Journal of Mechanical Engineering 71(2), pp. 151 – 166, **2021**. DOI: 10.2478/scjme-2021-0026

[10] Žiaran, S., Chlebo, O., Šooš, Ľ. "Determination of Bearing Quality Using Frequency Vibration Analysis", Strojnícky časopis – Journal of Mechanical Engineering 71(2), pp. 343 – 350, **2021**. DOI: 10.2478/scjme-2021-0040

[11] Shannon, C. E. “A Mathematical Theory of Communication”, The Bell System Technical Journal 27(3), pp. 379 – 423, **1948**. DOI: 10.1002/j.1538-7305.1948.tb01338.x

[12] Púčik, J., Oldřich, O., Elena, C. “Observability of Spectral Components beyond Nyquist Limit in Nonuniformly Sampled Signals”, International Scholarly Research Notices 2012, pp. 1 – 10, **2012**. DOI: 10.5402/2012/643563

[13] George, B. A., Hans, J. W., Frank, E. H. “Mathematical Methods for Physicists”, 7th edition, Academic Press, Waltham, USA, **2013**. ISBN: 9780123846549

[14] Wiener, N. “Generalized Harmonic Analysis”, Acta Mathematica 55, pp. 117 – 258, **1930**. DOI: 10.1007/BF02546511

[15] Khintchine, A. “Korrelationstheorie der stationären stochastischen Prozesse”, Mathematische Annalen. 109 (1), pp. 604 – 615, **1933**. DOI: 10.1007/BF01449156